

Polypyrrole – porous silicon nanocomposites

C. POPA^{a*}, R. TURCU^b, I. CRACIUNESCU^b, A. NAN^b, M.L. CIUREA^c, I. STAVARACHE^c, V. IANCU^d

^aTechnical University, Cluj-Napoca 3400, Romania

^bNational Institute for Research and Development of Isotopic and Molecular Technologies, Cluj-Napoca 5, 400293 Romania

^cNational Institute for Research and Development of Materials Physics, Bucuresti-Magurele 077125, Romania

^dUniversity “Politehnica” of Bucharest, Bucharest 060042, Romania

In this work we report the synthesis and characterization of the polypyrrole – porous silicon nanocomposites. Our main goal is to control the growth of conducting polypyrrole into the alveolar pores of porous silicon, in order to get a functionalized nanocomposite with the required properties for application as electrode in microfluidic devices. Porous silicon was electrochemically etched from (100) p-type silicon wafers. Different silicon resistivities (from 1.8 to 11 $\Omega\text{-cm}$) and preparation conditions (different electrolyte concentrations and current densities) were used. The electrodeposition of polypyrrole into porous silicon was carried out galvanostatically, at a constant current density 2.5 mA/cm^2 from a solution containing acetonitrile, the monomer, pyrrole and p-toluenesulfonic acid as electrolyte. The polymerization time was varied in order to investigate the growing process of polypyrrole into the pores. The morphology and of the as-prepared nanocomposites was investigated by SEM. The existence of PPy into porous silicon is evidenced by the EDX spectra of the nanocomposite. The electrical characterization evidences the relative contributions of the polypyrrole and the substrate resistivity, respectively.

(Received February 25, 2008; accepted August 14, 2008)

Keywords: polypyrrole, porous silicon, microfluidic devices

1. Introduction

The controlled selection of certain types of cells from a main blood stream is of particular importance for various medical applications, either for diagnostic or for the separation of stem, cancerous or infected cells. Two selection principles are employed: directly, using various field forces and indirectly, with coated magnetic nanobeads. Although the latter is highly accurate, as the beads are coated with specific antigens, the cost and the irreversibility of the cell – bead bind recommend the method only for diagnostic purposes. The direct approach is preferable when a subsequent re-use of the selected cells is targeted. An ideal example using a parallel array of two identical devices that select directly leukocytes is shown in Fig 1. Such a setting could be employed for the replacement of infected cells.

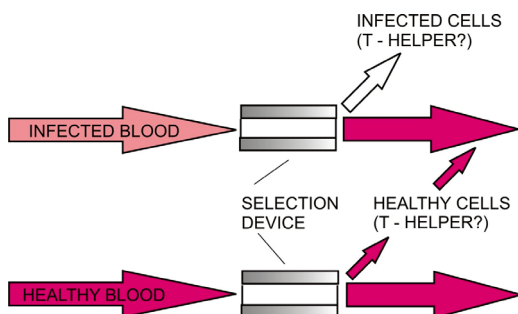


Fig.1 Direct selection devices used for the replacement of infected cells

Studied direct selection methods employ single force effects such as dielectrophoresis [1,2] and gravitational field flow fractionation [3,4], with a better resolution, techniques combining dual effects like mechanic / electrophoretic [5] or electrokinetic / magnetic (electromagnetophoretic) [6], or even more effects, for instance mechanic / electrokinetic / magnetic [7].

The polypyrrole properties like high electrical conductivity, relatively high environmental stability and biocompatibility [8] make this material suitable as electrode in microfluidic devices and biosensors.

In previous paper [9] we reported on the phototransport and photoluminescence in nanocrystalline porous silicon.

The present work presents a new concept of material to be used as bioelectrodes in dielectrophoretic microfluidic devices designed for the selection of leukocytes. The chip is made of porous silicon and the biosurface is of polypyrrole (PPy), electrochemically grown on the substrate.

2. Experimental

The electrodeposition of polypyrrole into porous silicon [9] was carried out at room temperature galvanostatically, at a constant current density $j = 2.5 \text{ mA/cm}^2$ from a solution containing acetonitrile, 0.1M pyrrole and 0.05M p-toluenesulfonic acid as electrolyte. A platinum wire was used as counter electrode.

The electrochemical growth of PPy was performed into porous silicon (PS) samples prepared in different conditions:

- PS2 : $\rho = 9 - 11 \Omega \text{ cm}$; HF : $\text{C}_2\text{H}_5\text{OH}$ (37,5 % : 62,5 %)
- PS3 : $\rho = 7 \Omega \text{ cm}$; HF : $\text{C}_2\text{H}_5\text{OH}$ (1 : 1); $t_a = 1 \text{ h } 20'$.

The nanocomposites polypyrrole-porous silicon (PPy/PS) were investigated by scanning electron microscopy (SEM) using a JSM 5600 LV JEOL microscope and EDX spectrometry (Oxford Instruments).



Fig. 2 Experimental microfluidic device.

The PPy/PS bioelectrodes were used in devices such as the one shown in Fig. 2, presented schematically in Fig. 3. The wafers are sealed on their PPy side with rubber and face a counterelectrode made of c.p. titanium.

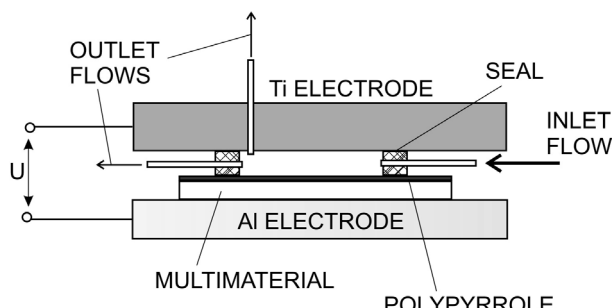


Fig. 3. Schematic design of the testing device

This electrode is also passed by one of the outlet tubes for the blood cells. Blood samples passed through the devices, with / without applying an electric potential (U). The signal shape was square (50%), with a frequency of 20 kHz and amplitude of 20 – 50 V, leading to a 13 – 33 V/m electric field. Due to the rough PPy surface that faces the smooth titanium counter electrode, the electric field is uneven, as shown in Figure 4. This leads to the occurrence of dielectric forces that act upon polarisable particles such as blood cells that pass between the electrodes.

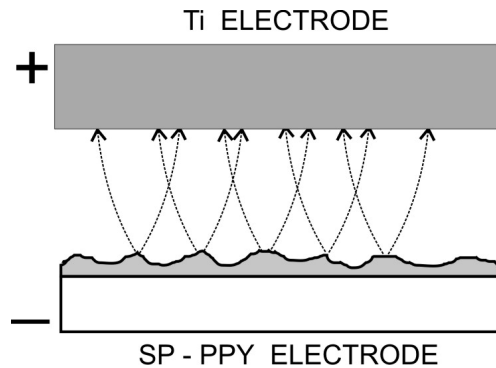


Fig. 4. Uneven electric field between electrodes

Sheep blood was used immediately after vein puncture and heparination. Blood samples were collected at the two outlets and smears were obtained in triplicate. After Giemsa staining, the smears were analysed by the blind method.

3. Results and discussion

The SEM images of the surface of nanocomposites samples PPy/PS2 and PPy/PS3 respectively are shown in the Figs. 5-8. As one can see from the Figs. 5 and 6 polypyrrole covers partially the surface of porous silicon. The sample PPy/PS2 shows a higher degree of covering of porous silicon by the polymer as compared with PPy/PS3.

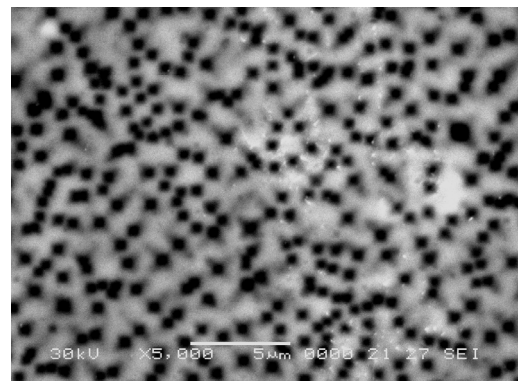


Fig. 5 SEM image of nanocomposite sample PPy/PS2 (PPy electropolymerization conditions: $j=2.5 \text{ mA/cm}^2$, $t=300\text{s}$).

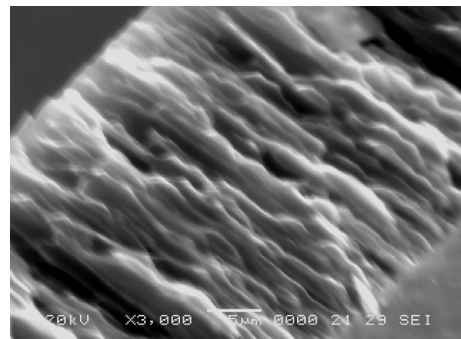


Fig. 6 SEM image of nanocomposite sample PPy/PS2 (fracture).

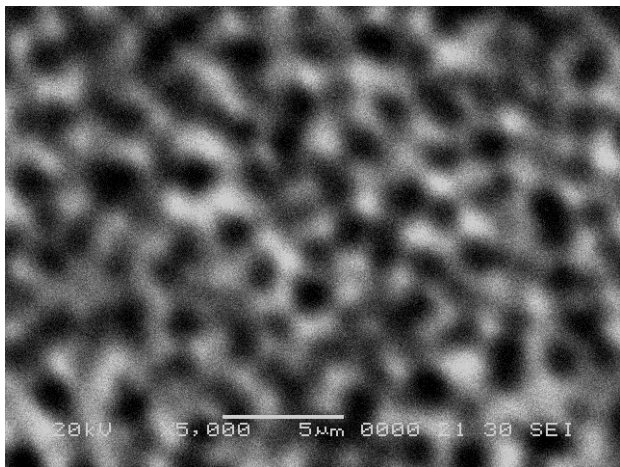


Fig.7 SEM image of nanocomposite sample PPy/PS3 (PPy electropolymerization conditions: $j=2.5 \text{ mA/cm}^2$, $t=300\text{s}$).

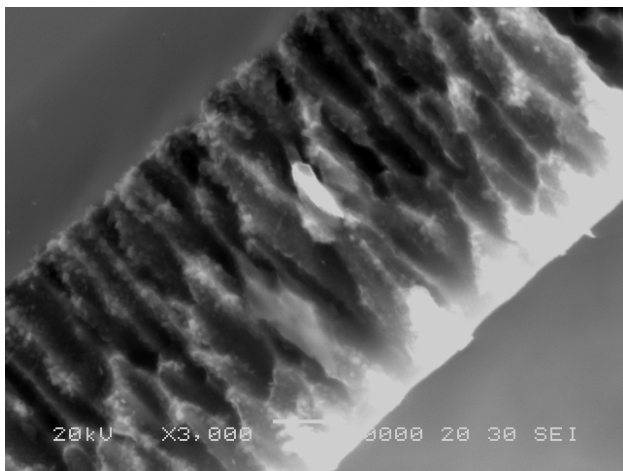


Fig.8 SEM image of nanocomposite sample PPy/PS3 (fracture).

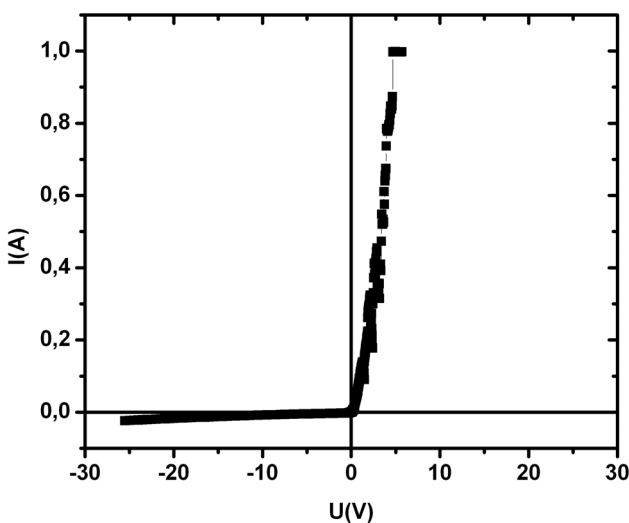


Fig.9 $I - V$ characteristic for PPy-PS sample

The growth of PPy onto the alveolar pore walls of porous silicon can be observed in Fig. 8 showing the characteristic globular morphology of PPy.

The $I - V$ characteristic shows a strongly rectifying behavior (Fig. 9). The current is 5 – 6 orders of magnitude greater than the values measured at the same bias on nanocrystalline PS [11,12]. This is due to the fact that the PPy enters all along the macropores and therefore shunt the PS. The rectifying behavior corresponds to the PPy/c-Si junction.

In order to evidence the specific features of the characteristic for both forward and reverse biases, we present them separately in Figs. 10 and 11. The reverse bias characteristic has no special behavior. On the contrary, the forward characteristic presents a number of strong oscillations, at 1.5, 2.5, 3.25, 4.0, and 4.7 V. These oscillations are typical for the percolation phenomena. Therefore one can conclude that the PPy columns from the PS macropores are not homogeneous, but present bottlenecks.

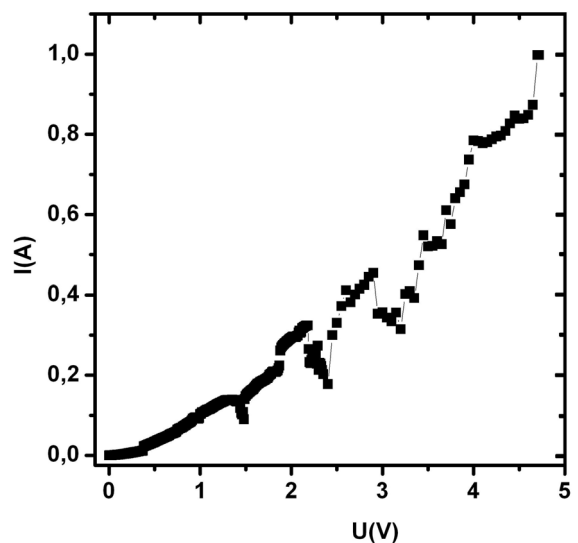


Fig.10 $I - V$ characteristic (forward bias).

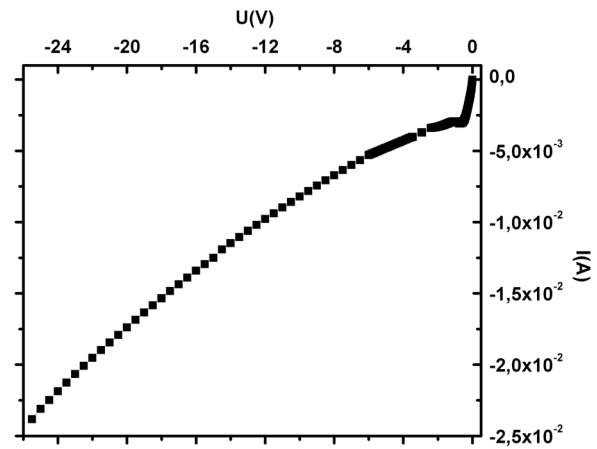


Fig.11 . $I - V$ characteristic (reverse bias).

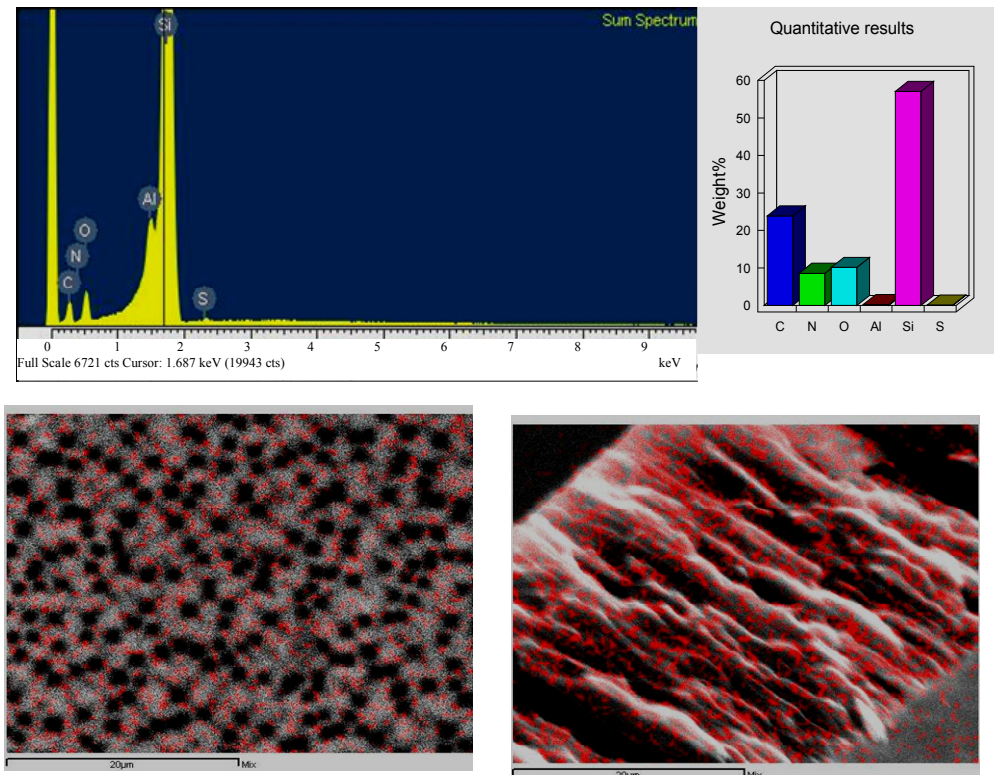


Fig.12 EDX spectrum of nanocomposite PPy/PS2, relative quantitative analysis for the main elements and the map distribution of carbon atoms.

EDX spectrum of the nanocomposite and the map distribution of carbon atoms given in the Fig. 12 demonstrate the formation of PPy into the porous silicon.

The nanocomposites PPy-PS were used as bioelectrodes in microfluidic devices for the selection of leukocytes.

The biologic results reveal the influence of the electric field parameters on the aspect of leukocytes and on the number of sampled cells at the two outlet tubes.

The aspect of eosinophils is agglutinated even for a 20V signal, Fig. 13, mainly for the PPy/PS electrode. This combination of parameters is not affecting on the aspect of the cells that are collected at the counterelectrode, Fig. 14. On the other hand, the concentration effect at the counterelectrode alters the aspect of the smears, giving the impression of monocytosis.

By increasing the amplitude of the electric signal, the aspect of neutral polymorphonuclears (NPMN) starts also to be affected at the SP-Ppy electrode. Fig. 15 shows an eosinophil without characteristic granulations, as well as a NPMN with a vital shape but pale after staining.

The aspect of cells at the counterelectrode can be altered for 35V, Fig. 16. In the case of 50V, all leukocytes, excepting lymphocytes, display a certain degree of shape altering, Fig. 17.

We can conclude that the increase in the signal amplitude is affecting first the eosinophils, than the NPMN and monocytes, while lymphocytes are the most resilient.

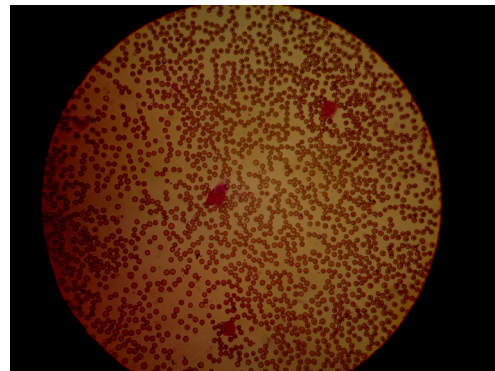


Fig. 13 Agglutinated eosinophil, SP-Ppy electrode; 20V

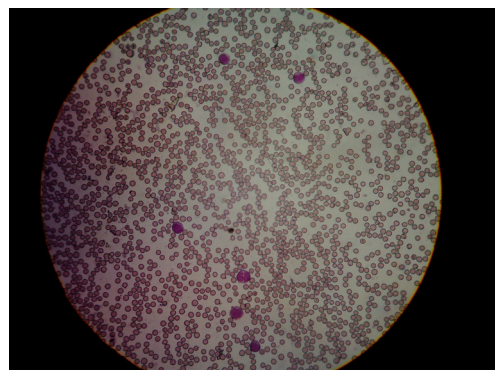


Fig. 14 Monocytes and lymphocytes with normal shape, aspect of monocytosis, counter electrode; 20V

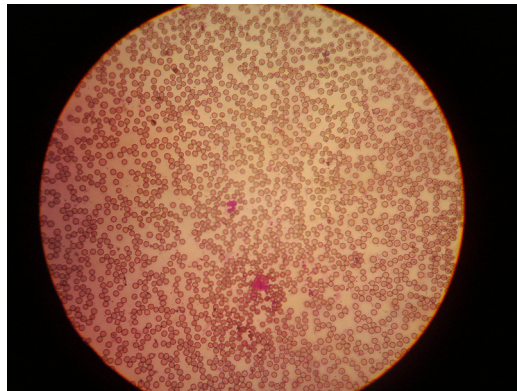


Fig.15 Eosinophils without granulations and pale NPMN, PPy/PS electrode; 35V.

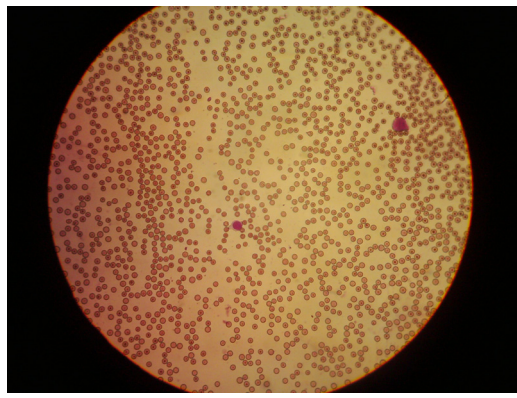


Fig.16 Epithelialized monocyte, counter electrode, 35V

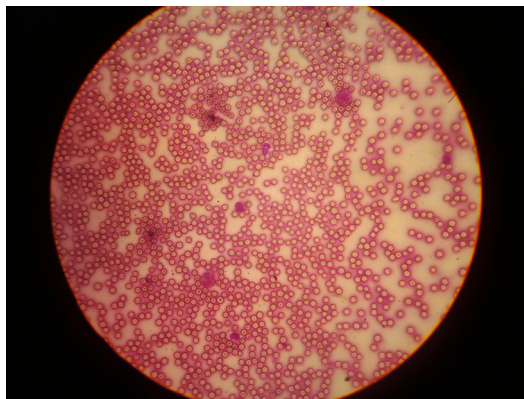


Fig.17. NPMN, monocyte and eosinophil in various altering stages, counterelectrode; 50V.

Figs. 18 – 21 show the variation of the number of leukocyte types sampled at the two outlets.

The difference in the dielectrophoretic force for the different classes of leukocytes is obvious considering the sampling site. For instance, the number of eosinophils is increasing with the voltage at the PS-Ppy work electrode, Figure 13, while at the counterelectrode it remains lower than initially, Figure 14. The lymphocytes are repelled by the counterelectrode, Figure 15, while monocytes are consistently concentrated by it, Figure 16.

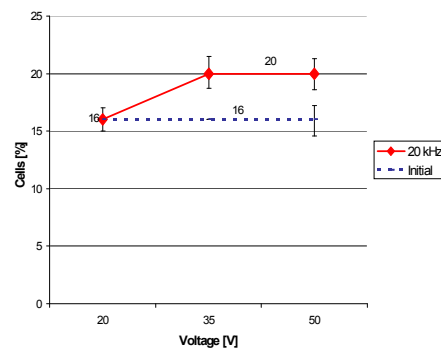


Fig.18 Number of eosinophils, PPy/ PS- electrode

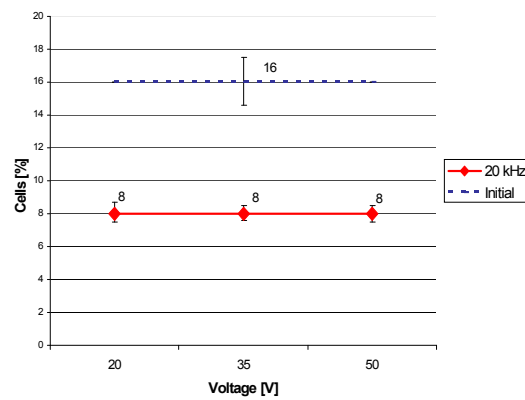


Fig.19 Number of eosinophils counterelectrode

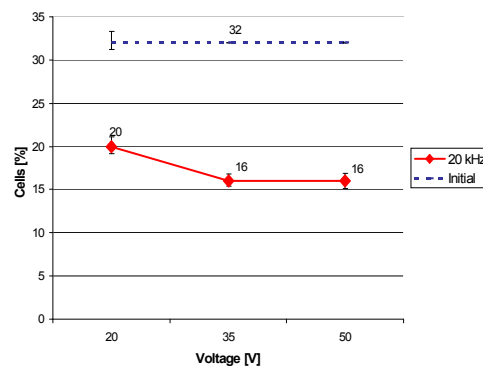


Fig.20 Number of lymphocytes, counterelectrode

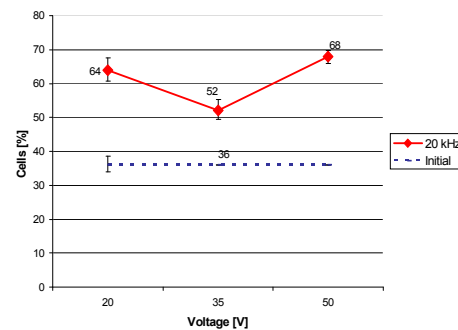


Fig.21 Number of monocytes, counterelectrode

If considering the behaviour of the leukocyte classes, one can conclude:

- Eosinophils display the most positive dielectrophoresis; are collected at the PS - Ppy electrode and repelled by Ti counterelectrode

- Neutral polymorphonuclears show an inconsistent response; are repelled by the PS - Ppy electrode but

problems occur in collecting at the counterelectrode, probably due to the shape in flow;

- Monocytes display a relatively negative dielectrophoresis, thus are collected at the counterelectrode;

- Lymphocytes show a relatively positive dielectrophoresis.

Thus, considering both the dielectrophoretic response and the sensitivity in the electric field, this experimental setting can be employed for the collection of viable lymphocytes at the PS-Ppy electrode and of monocytes at the counter electrode.

4. Conclusion

Porous silicon – polypyrrole bioelectrodes were produced in order to be used in dielectrophoretic microfluidic devices designed for the selection of leukocytes.

The morphology / electric properties of both PS substrate and multimaterial are suitable for the use as bioelectrodes, with possible sensing abilities.

Electric signals in the range of 10^5 V/m amplitude, with 20kHz frequency, are effective in the selection of eosinophils, lymphocytes or monocytes.

The morphology / viability of leukocytes is affected differently, according to the applied frequency / voltage.

References

- [1] X.B. Wang, J. Yang, Y. Huang, J. Vykovakal, F. F. Becker, P.R.C. Gascoyne, Cell Separation by Dielectrophoretic Field-flow-fractionation, *Analytical Chemistry*, **72**, 832 (2000).
- [2] J. Auerswald, H.F. Knapp, Quantitative assessment of dielectrophoresis as a micro fluidic retention and separation technique for beads and human blood erythrocytes, *Microelectronic Engineering*, **67**, 879 (2003).
- [3] D. Melucci, B. Roda, A. Zattoni, S. Casolari, P. Reschiglian, A. Roda, Field-flow fractionation of cells with chemiluminescence detection, *Journal of Chromatography A*, **1056**, 229 (2004).
- [4] S. Rasouli, E. Assidjo, T. Chianea, P.J.P. Cardot, Experimental design methodology applied to the study of channel dimensions on the elution of red blood cells in gravitational field flow fractionation, *Journal of Chromatography B*, **754**, 11 (2001).
- [5] G.J. Wang, W.H. Hsu, Y.Z. Chang, H. Yang, Centrifugal and electric field forces dual-pumping CD-like microfluidic platform for biomedical separation, *Biomedical Microdevices* **6**:1, 47 (2004).
- [6] Y. Iiguni, M. Suwa, H. Watarai, High-magnetic-field electromagnetophoresis of micro-particles in a capillary flow system, *Journal of Chromatography A*, **1032**(1-2), 165 (2004).
- [7] C. Popa, B. Su, P. Vadgama, F. Cotter, Magnetic Counter-Gravity Flow Separation of Electrically Pre-Polarised Lymphoid Cells, *British Journal of Haematology*, **136**(3), 433 (2006).
- [8] J. Rodriguez, H. J. Grande, T.F. Otero, *Handbook of Organic Conductive Molecules and Polymers*, Vol.2 Conductive Polymers: Synthesis and Electrical Properties, Ed. H.S. Nalwa, John Wiley 1997, p. 453.
- [9] V. Iancu, M. L. Ciurea, I. Stavarache, V. S. Teodorescu, *J. Optoelectron. Adv. Mater.* **9**(8), 2638 (2007).
- [10] M. L. Ciurea, C. Popa, and V. Iancu, Preparation of porous silicon layers: from micro to nano, *J. Optoelectron. Adv. Mater.* (in press).
- [11] M. L. Ciurea, I. Baltog, M. Lazar, V. Iancu, S. Lazanu, E. Pentia, Electrical behaviour of fresh and stored porous silicon films, *Thin Solid Films*, **325**, 271 (1998).
- [12] M. L. Ciurea, V. Iancu, V. Teodorescu, L. Nistor, M. G. Blanchin, Microstructural aspects related to carriers transport properties of nanocrystalline porous silicon films, *J. Electrochem. Soc.*, **146**(9), 3516 (1999).

* Corresponding author: catalin.popa@stm.utcluj.ro